Biobased Rigid Polyurethane Foam Prepared from Apricot Stone Shell-based Polyol for Thermal Insulation Application, Part 1: Synthesis, Chemical, and Physical Properties

Muhammed Said Fidan * and Murat Ertaş

Polyurethane foam is one of the most versatile construction insulation materials because of its low density, high mechanical properties, and low thermal conductivity. This study examined biobased rigid polyurethane foam composites from apricot stone shells, which are lignocellulosic residues. The apricot stone shells were liquefied with a PEG-400 (polyethylene glycol-400) and glycerin mixture in the presence of sulfuric acid catalyst at 140 to 160 °C for 120 min. Rigid polyurethane-type foam composites from the reaction were successfully prepared with different chemical components. Biobased polyurethane-type foam composites were successfully produced from the liquefied apricot stone shells. The FTIR spectra of liquefaction products confirmed successful liquefaction of products and that they are sources of hydroxyl groups. The liquefaction yield (81.6 to 96.7%), hydroxyl number (133.5 to 204.8 mg KOH per g), the highest elemental analysis amount (C, H, N, S, O) (62.08, 6.32, 6.12, 0.13, and 25.35%), and density (0.0280 to 0.0482 g per cm^3) of the rigid polyurethane foam composites were comparable to foams made from commercial RPUF composites.

Keywords: Polyurethane foam; Apricot stone shell; Liquefaction; Biobased polyol; Thermal insulation

*Contact information: Department of Forest Industry Engineering, Faculty of Forestry, Bursa Technical University, 16310, Bursa, Turkey; * Corresponding author: said.fidan@btu.edu.tr*

INTRODUCTION

Polyurethanes form a large polymer product family within the plastics group. Their consumption has been roughly 3 million tons per year in Europe throughout the 21st century. It consists of approximately 0.7 million tons of rigid PU foam, 1.8 million tons of flexible PU foam, 0.4 million tons of the PU elastomer, and other products (Mounanga *et al.* 2008).

Rigid polyurethane foams (RPUFs) are one of the most consumed polymeric materials. RPUFs have various applications in building insulation, construction, automobile industry, domestic appliances, transportation, and many others because of their low thermal conductivity, high closed-cell content, good shock absorption, low weight, and high strength (Polak *et al.* 2016; Akdogan *et al.* 2019). Moreover, the benefits of using an insulation material for optical instrument transformers (OITs) have led to the investigation of RPUFs for high voltage insulation purposes (Karady *et al*. 2003).

As can be seen in Fig. 1, RPUFs can be produced through interaction between polyols and polyisocyanate *via* poly addition polymerization (Acemioğlu *et al.* 2018). The polyurethane foam industry is mostly based on petro-based chemicals owing to its two

major feedstocks, *i.e.*, polyol and isocyanate. With the rapid depletion of fossil fuels and the increasing concern over environmental impacts, several effects have been concentrated on the substitution of petro-based polyols with biobased polyols. For example, bio-polyol and vegetable oil (Wang *et al.* 2008; Song *et al.* 2009; Zhang and Kessler 2015; Huang *et al.* 2017a) derived from lignocellulosic biomass have been studied (Xie *et al.* 2014; Huang *et al.* 2017a,b).

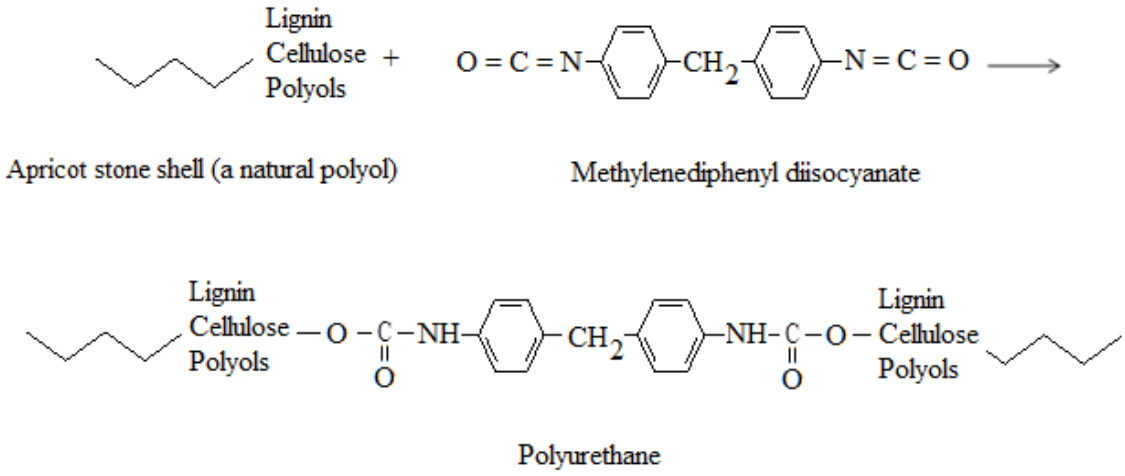

Fig. 1. Formation of RPUFs from the chemical reaction between apricot stone shell and MDI

Liquefaction is one of the thermochemical transformation methods that has been used to change lignocellulosic biomass into prized chemicals (Huang *et al.* 2017a). Such materials usually can be classed as agricultural wastes or residues of forest origin (Acemioğlu *et al.* 2019). The supreme molecular weight ingredients of biomass are broken down to drop the molecular chemical products. Various biomass conversion technologies have received growing attention. Thermochemical methods such as liquefaction and pyrolysis have great potential to produce biofuels and valuable bio-chemicals. Studies have shown that liquefaction provides an efficient pathway to convert solid biomass into liquid products (Xie *et al.* 2015). One major application of the liquefaction product is to produce the biobased polyurethane foam composites (Xie *et al.* 2014). The biofoams obtained from the liquefaction of lignocellulosic biomass are comparable to petro-based ones (Gama *et al.* 2015a).

Until recently, a considerable amount of biomass has been liquefied to produce biobased PU foams such as agricultural wastes, *e.g.*, corn bran (Lee *et al.* 2000), waste paper (Lee *et al.* 2002), chestnut and pine wood (Alma *et al.* 2003), cornstalk (Yan *et al.* 2008), wheat straw (Chen and Lu 2009), sugar-cane bagasse (Hakim *et al.* 2011), soybean straw (Hu *et al.* 2012), wood bark (Zhao *et al.* 2012), peanut shell (Bilir *et al.* 2013), wood powder (Zhang *et al.* 2013), bamboo (Xie *et al.* 2014), corn stover (Hu and Li 2014), eucalyptus and pine woods (Ertaş *et al.* 2014), cork (Gama *et al.* 2015b), lignin (Xue *et al.* 2015), coffee grounds (Gama *et al.* 2015a), sugar-cane bagasse (Xie *et al.* 2015), lignin (Mahmood *et al.* 2016), cork (Esteves *et al.* 2017), yaupon holly (Huang *et al.* 2017a), cotton burrs (Fidan and Ertaş 2020), and pine bark and peanut shell (Zhang *et al.* 2020). However, up to now there has been no research on the production of PU foam from the liquefaction of low-diameter apricot stone shells.

The rapid growth and wide distribution of apricot stone shell can continue to supply

lignocellulosic biomass. Apricot stone shell is one of the most widespread species in southeastern Turkey. It has a great potential to be used as a raw material for producing biofoam insulation composites via liquefaction.

In this study, PEG-400/glycerine was chosen as the liquefying agent because it is more environmentally friendly and economical than others. It also has a higher rate of liquefaction. Nevertheless, apricot stone shell was preferred because of its wide use.

The aim of this study was to utilize the apricot stone shells as polyols in the preparation of biobased rigid polyurethane foam insulation composites. The liquefaction parameters of apricot stone shell were optimized through the liquefaction and Fourier transform infrared (FTIR) spectrometry. Chemical properties (moisture, ash, extractives, cellulose, hemicellulose, lignin) and physical properties (density, particle size, color, elemental analysis) were determined.

EXPERIMENTAL

Materials

The apricot stone shell was collected at the Kahramanmaras Agricultural Research Institute in Kahramanmaras, Turkey. It was ground by a Wiley Laboratory Mill and passed through a 125 µm screen for the liquefaction experiments and then oven-dried at 105 °C until it reached a constant weight.

The powders (125 µm) of the apricot stone shell were used as primary natural polyols for making the polyurethane-type foams. In addition, polyethylene glycol (PEG 400), glycerol, sulfuric acid, and 1,4-dioxan (as of solvent) were reagent grade and were used without any further purification.

The components used to make the rigid polyurethane foam composites include diethylene glycol (DEG) as the commercial polyol, triethylene diamine (TEDA) as the foaming catalyst, silicon-glycol copolymer as a surfactant, and polymeric diphenylmethane diisocyanate (PMDI) as a crosslinking agent. Water was used as the environmentally friendly blowing agent. These ingredients were donated by the Nuhpol Polymer and Chemicals Industry Trade Stock Company in Turkey.

Methods

Liquefaction of the Biomass

Physical and chemical content of raw materials

Determinations of ash, moisture, cellulose, hemicellulose, lignin and extractives were made with NREL/TP-510-42622 (Sluiter *et al.* 2008a), NREL/TP-510-42621 (Sluiter *et al.* 2008b), Kurschner-Hoffner, and NREL/TP-510-42610 (Sluiter *et al.* 2008c) standards, respectively.

The process of liquefaction

The purpose was to convert the material used as apricot stone shell into a soluble form. The biopolyol from liquefied apricot stone shells for preparing RPUFc was attained using PEG/glycerol (4/1, weight per weight) with liquefaction solvents for 1, 1.5, and 2 h at 140, 160, and 180 °C. The liquid ratio and acid concentration was 3 to 1 (weight per weight) and 5, 7, and 9%, respectively (Table 1).

Table 1. Parameters of the Liquefaction

Number	Temperature (°C)	Time (min)	Amount of Acid-% (relate to solvent-g)	Apricot stone shell (g)	Rate of ASP/PEG 400-Glycerol	Rate of PEG-400+Gly. (g) (4 to 1)
1	140	120	9%–(2.7 g)	10	1/3	24+6
2	160	120	9%–(2.7 g)	10	1/3	24+6
3	180	120	9%–(2.7 g)	10	1/3	24+6
4	160	60	9%–(2.7 g)	10	1/3	24+6
5	160	90	9%–(2.7 g)	10	1/3	24+6
6	160	120	9%–(2.7 g)	10	1/3	24+6
7	160	120	5%–(1.5 g)	10	1/3	24+6
8	160	120	7%–(2.1g)	10	1/3	24+6
9	160	120	9%–(2.7 g)	10	1/3	24+6

Glycerol, PEG-400, and H_2SO_4 were added as determined by the prescribed composition required. They were loaded into a three-necked round bottom glass equipped with a reflux condenser and a stirrer. Apricot stone shell was added into the bottom glass, which was preheated to the desired temperature. The liquefaction was carried out with steady stirring at 140, 160, and 180 °C. After a given time, the reactor was quickly cooled to room temperature.

The reaction was concentrated by thin film evaporation at 60 °C to remove the binary solvent (dioxane/water ratio was 4 to 1). Afterwards, it was filtered through filter paper (Whatman No.4) to separate the solid and liquid residue. The amounts of unliquefied biomass were detected. The dioxane-water mixture was added to the liquefied specimen to detect the percent of soluble contents or the residue in dioxane.

Determination of percent dioxan-insoluble part

To determine the percent of dioxane-insoluble part attained at the end of liquefaction, the samples were diluted with 1,4-dioxane and filtered as described above. Ultimately, the percent dioxane-insoluble part (DIP) was determined according to Eq. 1,

$$DIP = (w_r \div w_{rm}) \times 100\ (\%) \quad (1)$$

where w_r is the weight of the residual (g) and w_{rm} is the weight of the raw material (g).

Determination of acid and hydroxyl values

The acid value was determined using a mixture of 1 g bio-polyol specimen and 20 mL dioxane-water solution (4 to 1, volume per volume). It was titrated with 0.1 mol per L of sodium hydroxide (NaOH) to pH 8.3 using a pH-meter to demonstrate the end-point. The blank titration was conducted using the same procedure. The acid value was calculated according to Eq. 2,

$$Acid\ value = [(C - D) \times N \times 56.1] \div W\ (\text{mg KOH per g}) \quad (2)$$

where C is volume of the sodium hydroxide standard solution consumed in the specimen titration (mL), D is volume of the sodium hydroxide standard solution consumed in the blank titration (mL), W is the specimen weight (g), and N is the equivalent concentration of the sodium hydroxide standard solution-mol per L (Wu *et al.* 2009; Huang *et al.* 2017).

The hydroxyl value was determined by weighing 1 g of the bio-polyol specimen into a 150 mL beaker. 10 mL of the phthalic anhydride solution (dissolving 150 g of phathalic anhydride in 900 mL of dioxane and 100 mL of pyridine) was added into the beaker. This beaker was sealed and put into a boiling water bath for 20 min. After cooling down, 20 mL of dioxane-water solution (4 to 1, volume per volume) and 5 mL of water was added to the beaker. It was then titrated with 1 mol per L of sodium hydroxide to pH 8.3 by using a pH-meter to demonstrate the end-point. The blank titration was conducted using the same procedure. The hydroxyl value was calculated according to Eq. 3,

$$Hydroxyl\ value = [(B - S) \times N \times 56.1 \div W] + AV \text{ (mg KOH per g)} \quad (3)$$

where B is the volume of the sodium hydroxide standard solution consumed in the blank titration (mL), S is the volume of the sodium hydroxide standard solution consumed in the sample titration (mL), W is the specimen weight (g), N is the equivalent concentration of the sodium hydroxide standard solution-mol per L, and AV is the acid value (Wu *et al.* 2009; Huang *et al.* 2017a).

Preparation of Rigid Polyurethane Biofoam Composites (RPUFc)

The sample that gave the best percentage of liquefaction was selected for the RPUFc production. Prior to the RPUFc production, the prepared biopolyols were neutralized with a NaOH solution.

A mixture of 50 g of liquefied biopolyols, 3.5 g of surfactants, 5 g of foaming catalyst, 5 g of diethylene glycol, and 5 g of deionized water were uniformly premixed in a plastic beaker with a mechanical stirrer for 30 s (Table 2). A certain amount of polymeric diphenylmethane diisocyanate (37.5 g, 50 g, 62.5 g, and 75 g) was added to the premixed components and stirred at a speed of 4000 rpm for approximately 1 min. The RPUFc samples were allowed to freely swell. The samples were exposed to ambient conditions for 2 days before characterization. Characterization tests were performed on four types of foam (Foam Code: RPUFc-75, RPUFc-100, RPUFc-125, RPUFc-150) and synthetic foam (RPUFc) according to the rate of pMDI.

Table 2. Compositions of the RPUFc

Components	Parts of biopolyol by weight (wt%)
Biopolyol (amount of liquefaction)	100
Silicon glycol copolymer (surfactants)	7
Triethylene diamine (foaming catalyst)	10
Diethylene glycol (DEG)	10
Water	7
Polymeric diphenylmethane diisocyanate (PMDI)	75-150

Characterization of liquefaction products

The liquefaction products of RPUFc were examined by FTIR. The FTIR analysis was performed by a Bruker Tensor 37 spectrometer (Bursa, Turkey) equipped with an ATR accessory. A small number of samples was used in FTIR analysis. The FTIR measurements were analyzed in the range from 400 cm^{-1} to 4000 cm^{-1} with a spectral resolution of 4 cm^{-1}.

Characterization of RPUFc

The densities of the RPUFc specimens were determined by dividing the weight of the samples (30 by 30 by 30 mm^3) by the calculated volume, according to the ASTM D1622-08 (2008). Six replicates were made for each group.

The amounts of C, H, N, O, H, and S of the RPUFc samples were determined by an elemental analyzer. The sample weight was used (2 to 5 mg). The elemental analysis was performed using a Thermo Scientific Flash Smart 2000 instrument and a TCD detector (FlashSmart 2000, Thermoscientific, Germany) with a 950 °C reactor temperature and a 65 °C column oven temperature.

RESULTS AND DISCUSSION

Chemical Characterization

Table 3 demonstrates the average chemical composition of the apricot stone shell as a raw material.

The apricot stone shell, having a particle size of 125 μm, consists of 33.3% cellulose, 27.8% hemicellulose, 52.0% lignin. The chemical composition of apricot stone shells is in good agreement with other values reported in the literature (Öztürk, 1995; Bostancı 1987). Also, the color of RPUFc liquefied apricot stone shell was determined as brownish.

Table 3. Chemical Composition of the Raw Material

Components	(%) ± Sx
Moisture	3.09 ± 0.1124
Ash	1.29 ± 0.0553
Extractives (Alcohol-benzene)	0.65 ± 0.0692
Cellulose	33.29 ± 0.7600
Hemicellulose	27.81 ± 0.2516
Lignin	52.01 ± 0.4112

It has been determined that the amount of cellulose and ash content in the apricot stone shells have lower amounts than different materials in the literature. It can be said that these differences are caused by the genetic structure of the materials. Considering the values obtained in comparison to the values in the literature, it can be said that apricot stone shells are similar to coniferous trees in terms of ash and cellulose amounts.

Liquefaction Parameters

Figures 2 through 4 show the liquefaction content results obtained for the apricot stone shell liquefaction with regard to reaction temperature, reaction time, and acid concentration (H_2SO_4).

Figure 2 summarizes the impact of reaction temperature on the liquefaction content. According to the ANOVA, no significant ($p > 0.05$) difference on the liquefied content was found among the different temperatures. It was obvious that the liquefied yield rose remarkably as the temperature increased from 81.60% at 140 °C to 96.70% at 160 °C. With further increase in the reaction temperature (95.54% at 180 °C), the liquefied content slowly fell.

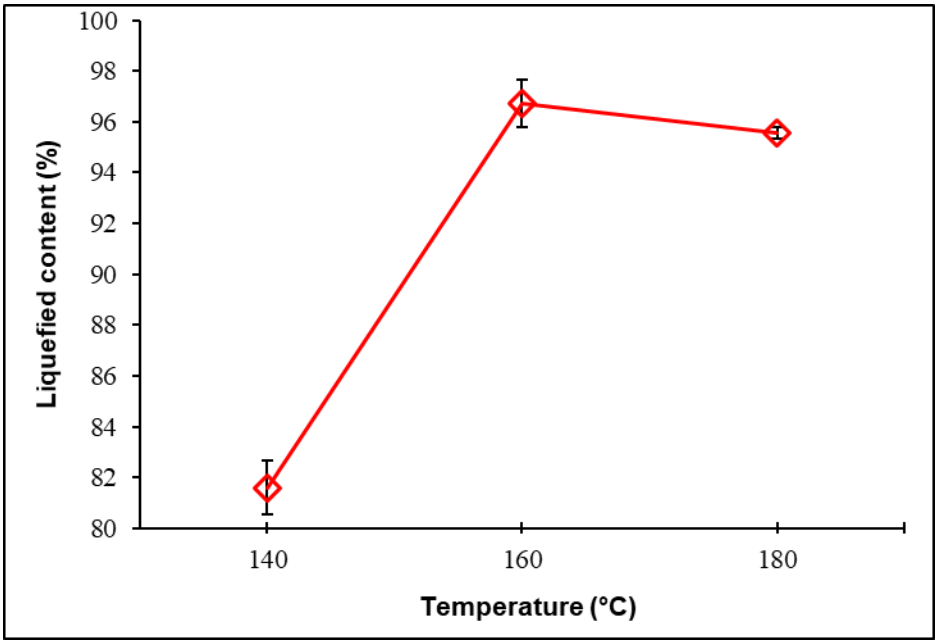

Fig. 2. The effect of reaction temperature on the liquefaction content (PEG 400/Glyserol: 4 to 1, ASP/Peg 400-Glyserol: 1 to 3, Acid concentration: 9%, Time: 120 min)

The results demonstrated that at temperatures higher than 160 °C the remaining lignocellulosic components were liquefied to some extent. The rise in liquefied yield during the initial period at a low temperature (140 °C and 160 °C) was fundamentally due to the fast degradation of the easily accessible apricot stone shell cell wall components. Some of the components were amorphous cellulose, hemicelluloses, and lignin (Zhang *et al.* 2012a; Huang *et al.* 2017a). Generally, the liquefaction of biomass is a dynamic balance between the recondensation of small liquefied fragments and the reactions of the decomposition in macromolecules (Xie *et al.* 2015; Esteves *et al.* 2017; Huang *et al.* 2017a). Therefore, by increasing the temperature from 140 °C to 180 °C, the quantity of activated macromolecules and their internal energy increased (Guo *et al.* 2012; Huang *et al.* 2017a). Thus, this caused more and more chemical bonds to be broken. As a consequence, the decomposition overweighed recondensation, which resulted in the rise of liquefied content (Zhuang *et al.* 2012; Huang *et al.* 2017b). When the reaction temperature was severe, the degradation gradually dropped and recondensation played a dominant role. This contributed to the decline of the liquefaction yield (Shao *et al.* 2016; Huang *et al.* 2017a). Therefore, 160 °C would be the most covetable liquefaction temperature for apricot stone shell.

Figure 3 demonstrates the alterations of the liquefaction amount as a function at various reaction times. According to the ANOVA, no significant ($p > 0.05$) difference in the liquefied content were found among the different reaction times. Expectedly, the liquefied amount increased as the reaction time increased, and the liquefaction efficiency increased with the rise of reaction time. As shown in Fig. 3, all the liquefaction yields of apricot stone shells were the highest at 96.7% for 120 min. Liquefied yields were determined from 95.5% at 60 min. to 96.4% at 90 min. The liquefied yield grew greatly with an increasing liquefaction time (Huang *et al.* 2017a). The increase of liquefaction yield was ascribed to the decomposition of amorphous zones of cellulose, hemicellulose, and lignin as they are vulnerable to the liquefaction process (Zhang *et al.* 2012a,b; Huang

et al. 2017a). The decomposition of the crystalline regions of cellulose made a contribution to the slow surge stage of liquefaction (Jasiukaityte *et al.* 2009; Huang *et al.* 2017a). In time, it was difficult for the solvent to penetrate the crystalline region of the cellulose, which decreased the reaction and dropped the liquefied yield. Furthermore, a long time and/or a high temperature could induce the recondensation of the already liquefied hemicellulose and lignin fragments (Xie *et al.* 2016). The side reactions of the decomposed cellulose may yield insoluble materials (Girisuta *et al.* 2006).

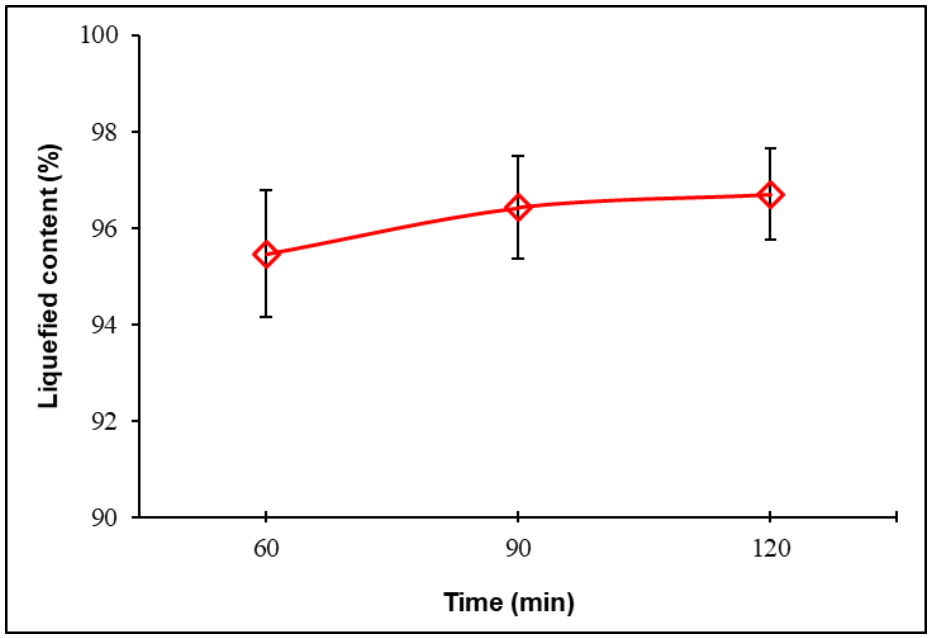

Fig. 3. The effect of reaction time on the liquefaction content (PEG 400/Glyserol: 4 to 1, ASP/Peg 400-Glyserol: 1 to 3, Temperature: 160 °C, Acid concentration: 9%)

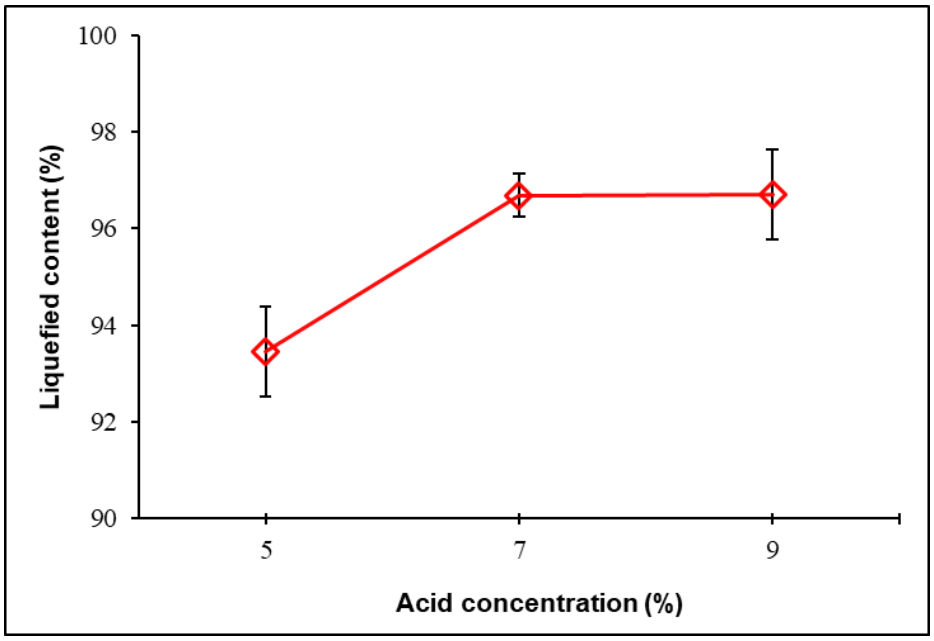

Fig. 4. The effect of acid concentration on the liquefaction content (PEG 400/Glyserol: 4 to 1, ASP/Peg 400-Glyserol: 1 to 3, Temperature: 160 ˚C, Time: 120 min)

The increased acid concentration had a positive impact on the liquefaction content of the apricot stone shells (Fig. 4). According to the ANOVA, no significant ($p > 0.05$) difference on the liquefied content was found among the different acid concentrations. The liquefied yield grew as the acid concentration (H_2SO_4) increased from 5% to 9%. The maximum conversion yield was observed at the acid concentration of 96.7% at 9%. The liquefied yields of acid concentration were determined as 93.5% at 5%, 96.7% at 7% and 96.7% at 9%, respectively. The rate of liquefaction gradually decreased with time as the acid concentration increased. This result was ascribed to recondensation among liquefied fragments with the excessive addition of H_2SO_4, which caused an increase in the insoluble residue (Zhang *et al.* 2012a; Lee *et al.* 2016; Huang *et al.* 2017a). Recondensation only happens when both the lignin and the cellulose are liquefied. However, according to the authors, this reaction can be inhibited by the addition of low-molecular weight glycols such as glycerol (Kurimoto *et al.* 1999). The use of glycerol limits the recondensation reactions and at the same time lowers the cost of the process since glycerol is less expensive than other polyalcohols. The possible use of crude glycerol in cork liquefaction could further decrease the cost of the process (Esteves *et al.* 2017). This concept was applied successfully in the liquefaction of soybean straw (Hu *et al.* 2012). Liquefaction yields increased as the reaction time was prolonged. Additional reaction time did not appreciably increase the liquefaction yield and would cause the process to be more expensive (Esteves *et al.* 2017). Consequently, the optimal liquefaction yield (96.7%) was accomplished at 160 °C for 120 min and 9% acid concentration. Alma *et al.* (2003) found that the amount of material that did not react was detected the lowest with 120 min in chestnut. Differences in amount of the residue content of cotton burr after liquefaction can be categorized by distances in structures and the types of hemicellulose and lignin of softwood and hardwood (Alma *et al.* 2003).

Acid and Hydroxyl Values

Figures 5 through 7 show the acid and hydroxyl value results obtained for the apricot stone shell liquefaction with regard to reaction temperature, reaction time, and acid concentration (H_2SO_4).

Figure 5 demonstrates the impact of reaction temperature on the acid and hydroxyl values. As the reaction temperatures were increased, the acid values were also increased, but the hydroxyl values were decreased. Figure 6 summarizes the alterations of the acid and hydroxyl values as a function at different reaction times. The acid value of the reaction times was within the range of 49.4 to 70.1 mg KOH per g. The hydroxyl value of the reaction times was 133.5 and 204.8 mg KOH per g, respectively. Expectedly, the rise of acid concentration had an affirmative impact on the hydroxyl and acid values of apricot stone shells (Fig. 7). The acid values remarkably increased as the acid concentration (H_2SO_4) increased from 5% to 9%. The maximum hydroxyl values were determined at the acid concentration of 195.2% at 5%.

The rise in acid number can be attributed to either the oxidation of the carbohydrates or the increase of acidic substances and lignin during the liquefaction. The increase in the hydroxyl number can be conceivably attributed to the cleavage of ether and ester or linkages between the lignin units. After that, the hydroxyl number dropped slowly (Chen and Lu 2009). This can be ascribed to oxidation reactions, dehydration, or alcoholysis of hydroxyl groups occurring during liquefaction.

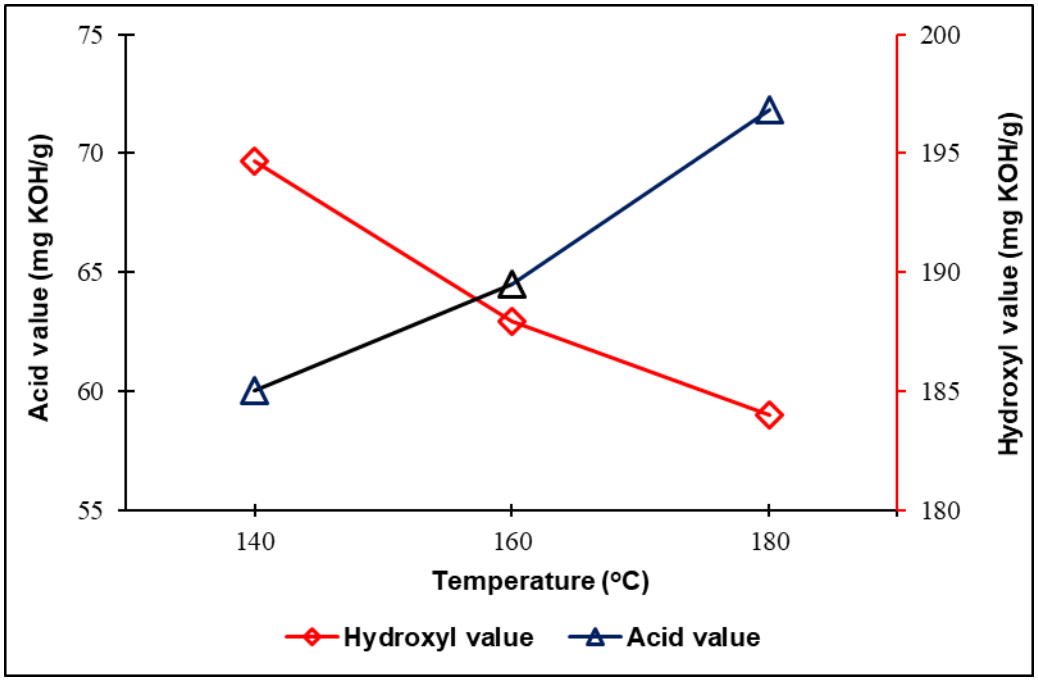

Fig. 5. The effect of reaction temperature on the acid and hydroxyl value

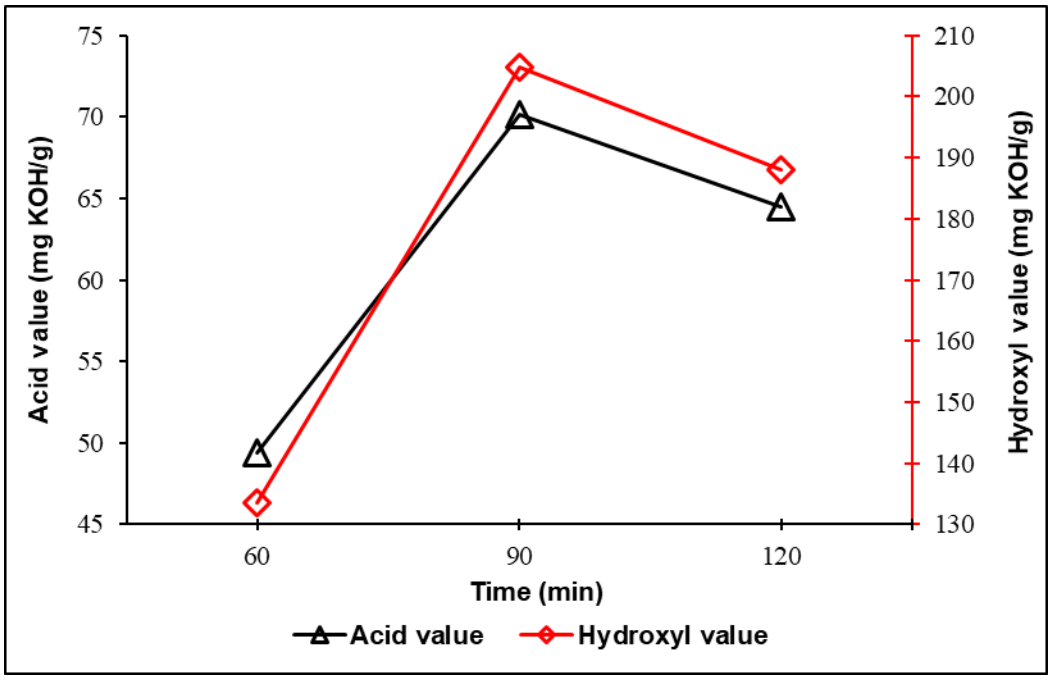

Fig. 6. The effect of reaction time on the acid and hydroxyl value

The hydroxyl value of the bio-polyols is an important parameter that needs to be monitored during bio-polyols and RPUF fabrication. Furthermore, high temperature contributed to the smaller hydroxyl values. This demonstrates that although the PA in the mixture can ensure the hydroxyl group of the bio-polyols, a loss of hydroxyl groups happened during the liquefaction reaction. This could be substantially contributing to the formation of ethers and the alcoholysis reaction. The decomposed bagasse components, the

oxidation reactions, and recondensation among the liquefaction solvents could have also occured during the liquefaction to use up the hydroxyl value and effect the hydroxyl groups. The higher hydroxyl amount for the bio-polyols from the reaction with high solvent loading may be due to the higher biomass conversion and that the extra solvent in the reaction mixture abstained the recondensation reactions. The bagasse was acidic due to the acid catalyst used in the liquefaction. In other respects, the acid component was a product of decomposition from the wood ingredients, mainly hemicellulose and cellulose (Xie *et al.* 2015).

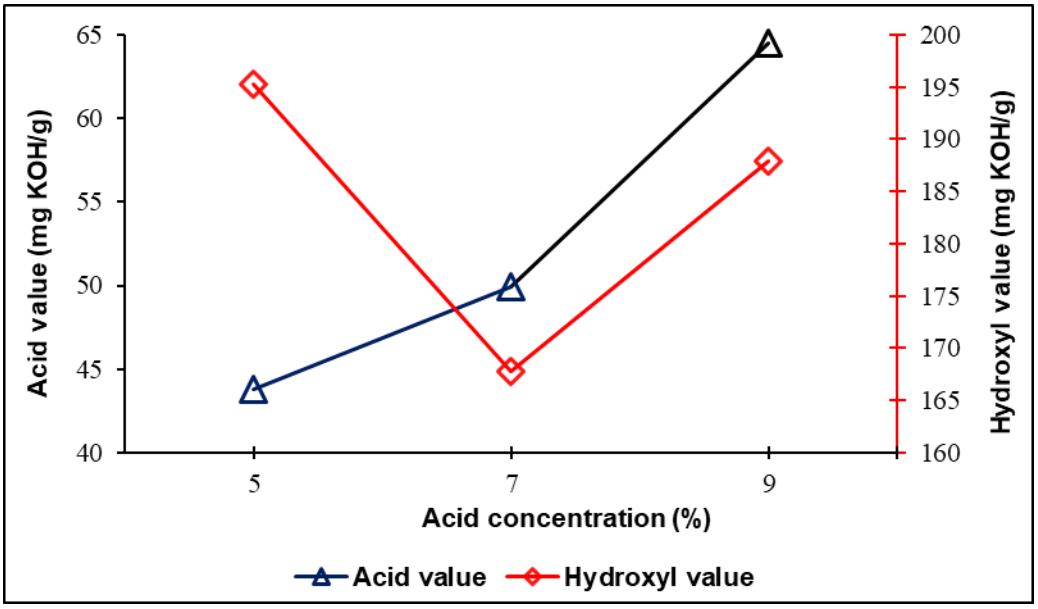

Fig. 7. The effect of acid concentration on the acid and hydroxyl value

FTIR Analysis of Liquefaction Products

Figure 8 compares the FTIR spectra of the original raw material (apricot stone shell), solid residue, bio-polyol, and liquefied apricot stone shell from post-liquefaction treatment (for a sample with a 96.7% liquefaction yield).

Several differences can be observed in the spectra that may ensure insights into the liquefaction process. Comprehensively, important differences were determined between the spectra of solid residue and the raw material, bio-polyol, and liquefied apricot stone shell. Differences among the spectra indicated that the structure of the main apricot stone shell polymers was modified by the liquefaction process. The band in the 3200 to 3450 cm^{-1} region is attributed to the non-bonded stretching vibrations of the O—H groups and the symmetric and asymmetric stretching vibrations of the N—H urea groups and urethane (Gama, 2015b; Huang *et al.* 2017c). It was clear that the macromolecules in lignocellulosic materials were broken down after liquefaction, which was evidenced from the observation of methyl (2917 cm^{-1}) and/or methylene (2872 cm^{-1}) in solid residue (Chen *et al.* 2014; Huang *et al.* 2017a; Esteves *et al.* 2017; Chen *et al.* 2019). The intensified -OH characteristic peak at around 3384 cm^{-1} was observed on the spectrum of solid residue (Huang *et al.* 2017a), which indicated that the hydroxyl groups in the raw materials were released through liquefaction.

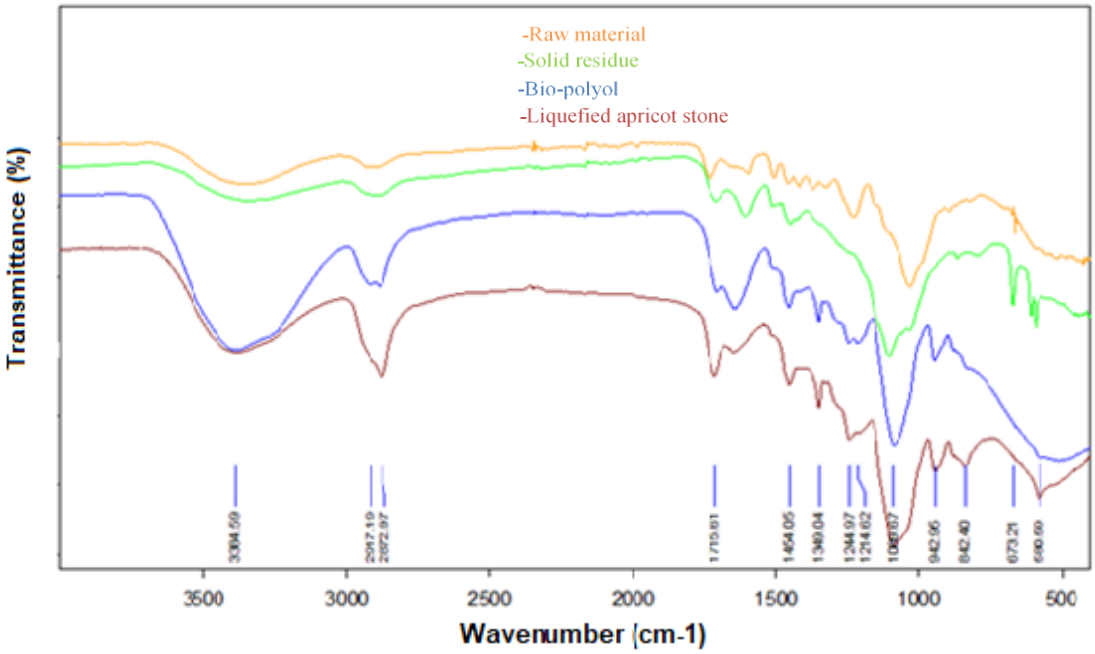

Fig. 8. FTIR spectra of the raw material, solid residue, bio-polyol, and liquefied apricot stone shell using the optimal liquefaction parameters

The strong hydroxyl group peaks in bio-polyol and liquefied apricot stone shell were relatively referred to the liquefaction solvent, *i.e.*, PEG and glycerol. The other part of the hydroxyl sources was derived from the liquefaction of the apricot stone shell.One of the hydroxyl sources is the liquefaction of hemicellulose, which can produce an abundance of C5 sugars with a multi-hydroxyl structure (Xu *et al.* 2016; Huang *et al.* 2017a,b). The prominent peaks appeared on the spectra of bio-polyol and liquefied apricot stone shell at 1715 cm^{-1} corresponding to the uronic ester and acetyl groups in hemicellulose (Li *et al.* 2015; Xie *et al.* 2015; Huang *et al.* 2017a), which suggested that the hemicellulose in the raw material was successfully liquefied and dissolved into bio-polyol. The liquefaction of cellulose is another hydroxyl source, which provides an abundance of C6 sugars that are rich in hydroxyl groups (Xu *et al.* 2016; Huang *et al.* 2017a,b). The liquefaction of cellulose could be observed by comparing cellulose characteristic peaks in liquefied apricot stone shell and solid residue at 1430 cm^{-1} ($C-H_2$), 1089 cm^{-1} (C-O), and 942 cm^{-1} (C-H) (Chen *et al.* 2014; Li *et al.* 2015; Huang *et al.* 2017a). The peaks at 1454 cm^{-1} (C-H in aromatic rings) and 1244 cm^{-1} (guaiacyl ring) are characteristic of lignin structures in both the liquefied material and the solid residue (Poletto *et al.* 2012; Li *et al.* 2015; Esteves *et al.* 2017; Huang *et al.* 2017a). These peaks were discovered in the spectra of liquefied apricot stone shell and bio-polyol, which indicated that the lignin in the raw material was successfully liquefied and decomposed into bio-polyol as well. Furthermore, the lignin-derived hydroxyl group was also observed in the bio-polyol at a peak of 1349 cm^{-1} (Alriols *et al.* 2009; Huang *et al.* 2017a). This group was also a hydroxyl source in the liquefaction of lignin.

Characterization Parameters of RPUFc

As shown in Fig. 9, the density of the RPUFc obtained in this study was determined

varying from 0.029 g per cm^3 to 0.048 g per cm^3. According to the ANOVA, no significant ($p > 0.05$) difference on the density was found among the different foam codes. As reported, the density of RPUF made from the liquefaction of biomass are in the range of 0.020 g per cm^3 to 0.125 g per cm^3 (Wu *et al.* 2009; Xie *et al.* 2014; Gama *et al.* 2015a; Xie *et al.* 2015; Gama *et al.* 2015b; Mahmood *et al.* 2016; Esteves *et al.* 2017; Huang *et al.* 2017a,b,c; Akdogan *et al.* 2019). In comparison to these RPUFs, the RPUFc obtained in this study show similar characteristics in line with the results in the literature.

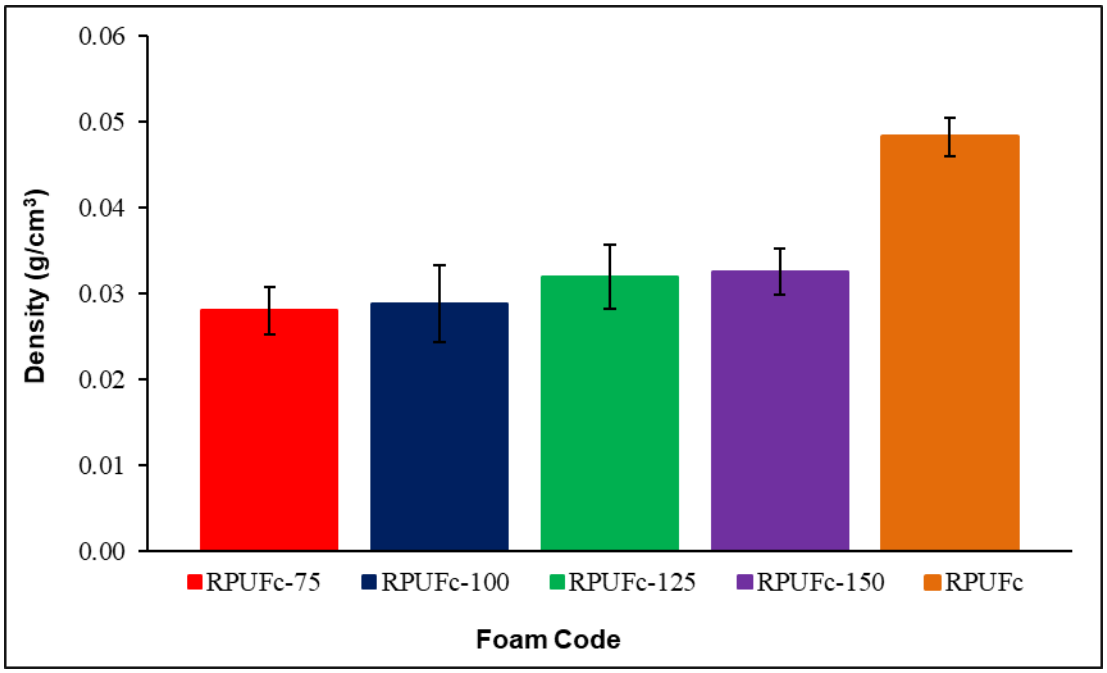

Fig. 9. The density of the RPUFc

The density of RPUFc increased with an increased polymeric diphenylmethane diisocyanate (pMDI) content from 75 to 150. To explain the impact of biopolyols amount on the RPUF density, it is necessary to demonstrate the reaction pathways between each pMDI and biopolyols material (Xie *et al.* 2014). In the meantime, density is an important property as it effects the mechanical properties and thermal conductivity of the RPUF (Gama *et al.* 2015b). The density was importantly dependent on the foam cell size. Density of the RPUF is known to drop as the cell diameter raises, which further effects the mechanical properties (Huang *et al.* 2017c; Akdogan *et al.* 2019). Generally, foam with a larger pore diameter will have a lower density and vice versa (Ugarte *et al.* 2014; Huang *et al.* 2017a).

As shown in Fig. 10, the amount of the raw marerial and RPUFc were determined through elemental analysis. The highest percentage of C, H, N, S, and O was determined to be 64.56% in RPUFc-125, 6.80% in RPUFc-75, 6.14% in RPUFc-125, 0.50% in RPUFc-75, and 49.84% in the raw material, respectively.

As shown in Fig. 10, the elemental analysis results of the raw material were found to be lower than the control sample (RPUFc). The amount of elemental analysis in RPUFc-75, RPUFc-100, RPUFc-125, and RPUFc-150 was higher than the raw material. Furthermore, the amount of raw material and control sample (RPUFc) were lower than RPUFc-75 and RPUFc-125.

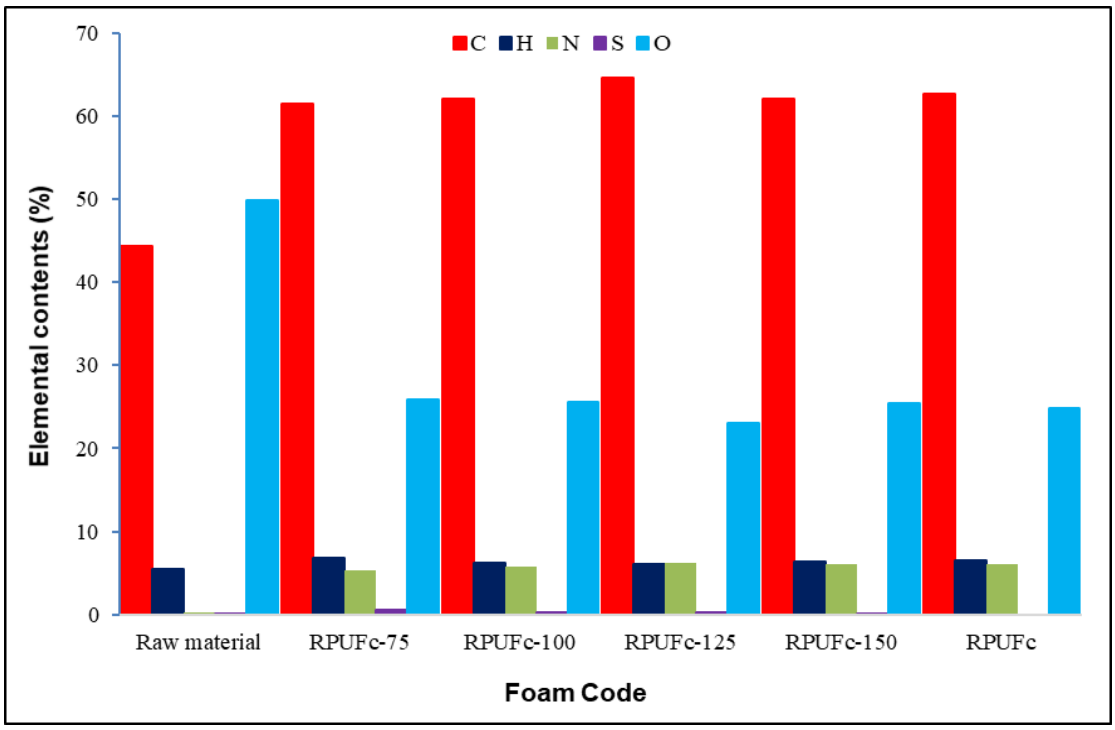

Fig. 10. Elemental analysis of the RPUFc

CONCLUSIONS

1. The results demonstrate that it is possible to liquefy a great rate of apricot stone shells with an acid catalysis, which can be used to produce rigid polyurethane foams.
2. The optimized liquefaction parameters include temperatures in the range of 140 to 160 °C, time in the range of 60 to 120 min, and acid concentration ratio set from 5 to 9%. The high liquefaction yield obtained from the apricot stone shells were indicated at 160 °C for 120 min and catalyzed by 9% H_2SO_4. The optimal liquefaction yield was 96.7%. The conversion yield remarkably grew with a raising liquefaction temperature, time, and acid concentration.
3. The FTIR spectra of liquefaction products confirmed the successful liquefaction of lignin, cellulose, and hemicellulose, and that they are sources of hydroxyl groups. The hydroxyl number of bio-polyol was 133.5 and 204.8 mg KOH per g was determined using a titration method.
4. The desired biobased RPUFc was obtained by controlling the pMDI ratio of 150%.
5. According to elemental analysis, the percentage of the highest C, H, N, S, and O content was determined to be 62.1%, 6.3%, 6.1%, 0.13%, and 25.4% in RPUFc-150, respectively.
6. The density of the resulting RPUFc was 0.0325 g per cm^3. The RPUFc obtained with the increase of the pMDI content resulted in a decline in comparison to the control samples in the apparent density.

7. Morphological, chemical, and physical property characterization results demonstrated that the foam properties influentially rely on the percentage of the physical blowing agent and the percentage of bio-contents in the apricot stone shell based polyols.

ACKNOWLEDGMENTS

The authors thank to Nuhpol Polymer and Chemicals Industry Trade Stock Company in Turkey for providing chemical samples.

REFERENCES CITED

Acemioğlu, B., Bilir, M. H., and Alma, M. H. (2018). "Adsorption of safranin-O dye by peanut shell-based polyurethane type foam," *International Journal of Chemistry and Technology* 2(2), 95-104. DOI: 10.32571/ijct.454516

Acemioğlu, B., Karataş, N., Güler, M. H., Ertaş, M., and Alma, M. H. (2019). "Adsorption of basic red 2 dye by activated biomass charcoal in batch and column systems," *International Journal of Chemistry and Technology* 3(2), 136-145. DOI: 10.32571/ijct.650476

Akdogan, E., Erdem, M., Ureyen, M. E., and Kaya, M. (2019). "Rigid polyurethane foams with halogen-free flame retardants: Thermal insulation, mechanical, and flame retardant properties," *Journal of Applied Polymer Science* 136, 47611, 1-14. DOI: 10.1002/app.47611

Alma, M. H., Basturk, M. A., and Dıgrak, M. (2003). "New polyurethane-type rigid foams from liquified wood powders," *Journal of Materials Science Letters* 22, 1225-1128

Alriols, M. G., Tejado, A., Blanco, M., Mondragon, I., and Labidi, J. (2009). "Agricultural palm oil tree residue as raw material for cellulose, lignin and hemicelluloses production by ethylene glycol pulping process," *Chemical Engineering Journal* 148(1), 106-114. DOI: 10.1016/j.cej.2008.08.008

ASTM D1622-08 (2008). "Standard test method for apparent density of rigid cellular plastics," ASTM International, West Conshohocken, PA

Bilir, M. H., Şakalar, N., Acemioğlu, B., Baran, E., and Alma, M. H. (2013). "Sorption of Remazol Brilliant Blue R onto polyurethane-type foam prepared from peanut shell," *Journal of Applied Polymer Science* 127(6), 4340-4351. DOI: 10.1002/app.37614

Bostancı, Ş. (1987). *Pulp Production and Bleaching Technology* (General Edition Number: 114), Faculty of Forestry, Trabzon, Turkey, pp. 32-33.

Chen, F., and Lu, Z. (2009). "Liquefaction of wheat straw and preparation of rigid polyurethane foam from the liquefaction products," *Journal of Applied Polymer Science* 111, 508-516. DOI: 10.1002/app.29107

Chen, C., Luo, J., Qin, W., and Tong, Z. (2014). "Elemental analysis, chemical composition, cellulose crystallinity, and FT-IR spectra of toona sinensis wood," *Monatshefte für Chemie* [Chemical Monthly] 145(1), 175-185. DOI: 10.1007/s00706-013-1077-5

Chen, X., Li, J., and Gao, M. (2019). "Thermal degradation and flame-retardant

mechanism of the rigid polyurethane foam including functionalized graphene oxide," *Polymers* 11, 78, 1-11. DOI: 10.3390/polym11010078

Ertaş, M., Fidan, M. S., and Alma, M. H. (2014). "Preparation and characterization of biodegradable rigid polyurethane foams from the liquefied eucalyptus and pine woods," *Wood Research* 59(1), 97-108. DOI: 10.15376/biores.12.4.8160-8179

Esteves, B., Dulyanska, Y., Costa, C., Vicente, J., Domingos, I., Pereira, H., Lemos, L. T., and Lopes, L.C. (2017). "Cork liquefaction for polyurethane foam production," *BioResources* 12(2), 2339-2353. DOI: 10.15376/biores.12.2.2339-2353

Fidan, M. S. and Ertaş, M. (2020). "Optimization of liquefaction parameters of cotton burrs (*Gossypium hirsutum* L.) for polyurethane-type isolation foams," *Kastamonu University Journal of Forestry Faculty* 20(1), 15-24.

Gama, N. V., Soaresa, B., Freirea, C. S. R., Silvab, R., Netoa, C. P., Timmonsa, A. B., and Ferreira, A. (2015a). "Bio-based polyurethane foams toward applications beyond thermal insulation," *Material Design* 76, 77-85. DOI: 10.1016/j.matdes.2015.03.032

Gama, N., Soares, B., Freire, C. S. R., Silva, R., Brandão, I., Neto, C. P., Timmonsa, A. B., and Ferreira, A. (2015b). "Rigid polyurethane foams derived from cork liquefied at atmospheric pressure," *Polymer International* 64, 250-257. DOI: 10.1002/pi.4783

Girisuta, B., Janssen, L. P. B. M., and Heeres, H. J. (2006). "A kinetic study on the decomposition of 5-hydroxymethylfurfural into levulinic acid," *Green Chemical* 8, 701-709. DOI: 10.1039/b518176c

Guo, J., Zhuang, Y., Chen, L., Liu, J., Li, D., and Ye, N. (2012). "Process optimization for microwave-assisted direct liquefaction of *Sargassum polycystum C.* agardh using response surface methodology," *Bioresource Technology* 120, 19-25. DOI:10.1016/j.biortech.2012.06.013

Hakim, A. A. A., Nassar, M., Emam, A., and Sultan, M. (2011). "Preparation and characterization of rigid polyurethane foam prepared from sugar-cane bagasse polyol," *Material Chemical Physics* 129(1-2), 301-307. DOI: 10.1016/j.matchemphys.2011.04.008

Hu, S., Wan, C., and Li, Y. (2012). "Production and characterization of biopolyols and polyurethane foams from crude glycerol based liquefaction of soybean straw," *Bioresource Technology* 103(1), 227-233. DOI: 10.1016/j.biortech.2011.09.125

Hu, S., and Li, Y. (2014). "Two-step sequential liquefaction of lignocellulosic biomass by crude glycerol for the production of polyols and polyurethane foams," *Bioresource Technology* 161, 410-415. DOI: 10.1016/j.biortech.2014.03.072

Huang, X. Y., Qi, J. Q., Hoop, C. F., Xie, J. L., and Chen, Y. Z. (2017a). "Biobased polyurethane foam insulation from microwave liquefaction of woody underbrush," *Bioresources* 12(4), 8160-8179. DOI: 10.15376/biores.12.4.8160-8179

Huang, X. Y., Li, F., Xie, J. L., Hoop, C. F., Hse, C. Y., Qi, J. Q., and Xiao, H. (2017b). "Microwave-assisted liquefaction of rape straw for the production of bio-oils," *BioResources* 12(1), 1968-1981. DOI: 10.15376/biores.12.1.1968-1981

Huang, X., DeHoop, C. F., Xie, J., Hse, C. Y., Qi, J., and Hu, T. (2017c). "Characterization of biobased polyurethane foams employing lignin fractionated from microwave liquefied switchgrass," *International Journal Polymer Science*, 8. DOI: 10.1155/2017/4207367

Jasiukaitytė, E., Kunaver, M., and Strlič, M. (2009). "Cellulose liquefaction in acidified ethylene glycol," *Cellulose* 16(3), 393-405. DOI: 10.1007/s10570-009-9288-y

Karady, G. G., Argin, M., Shi, B., Rahmatian, F., and Rose, A. H. (2003). "Electrical

properties of rigid pour polyurethane foam applied for high voltage insulation," *Proceedings of the IEEE Power Engineering Society Transmission and Distribution Conference* 3, 870-974

Kurimoto, Y., Doi, S., and Tamura, Y. (1999). "Species effects on wood liquefaction in polyhydric alcohols," *Holzforschung* 53, 617-622. DOI: 10.1515/HF.1999.102.

Lee, S. H., Yoshioka, M., and Shiraishi, N. (2000). "Liquefaction of corn bran (CB) in the presence of alcohols and preparation of polyurethane foam from its liquefied polyol," *Journal Applied Polymer Science* 7(2), 319-325. DOI: 10.1002/1097-4628(20001010)78:2<319::AID-APP120>3.0.CO;2-Z

Lee, S. H., Teramoto, Y., and Shiraishi, N. (2002). "Biodegradable polyurethane foam liquefied waste paper and its thermal stability, biodegradability, and genotoxicity," *Journal Applied Polymer Science* 83(7), 1482-1489. DOI: 10.1002/app.10039

Lee, J. H., Lee, J. H., Kim, D. K., Park, C. H., Yu, J. H., and Lee, E. Y. (2016). "Crude glycerol-mediated liquefaction of empty fruit bunches saccharification residues for preparation of biopolyurethane," *Journal Industrial and Engineering Chemical* 34, 157-164. DOI: 10.1016/j.jiec.2016.04.019

Li, G., Hse, C., and Qin, T. (2015). "Wood liquefaction with phenol by microwave heating and FTIR evaluation," *Journal Forest Research* 26(4), 1043-1048. DOI: 10.1007/s11676-015-0114-0

Mahmood, N., Yuan, Z., Schmidt, J., Tymchyshyna, M., and Xu, C. (2016). "Hydrolytic liquefaction of hydrolysis lignin for the preparation of bio-based rigid polyurethane foam," *Green Chemistry* 18, 2385-2398. DOI: 10.1039/c5gc02876k

Mounanga, P., Gbongbon, W., Poullain, P., and Turcry, P. (2008). "Proportioning and characterization of lightweight concrete mixtures made with rigid polyurethane foam wastes," *Cement Concrete Comp* 30, 806-814. DOI: 10.1016/j.cemconcomp.2008.06.007

Öztürk, E. (1995). *Determination of Pulp Production Conditions by Alkali-Sulfite-Anthraquinone-Ethanol (ASAE) Method from Cotton Stems (Gosipium hirsipum L.)*, MSc Thesis, Karadeniz Technical University, Institute of Natural Applied Sciences, Trabzon, Turkey.

Polak, J. C., Przybyszewski, B., Heneczkowski, M., Czulak, A., and Gude, M. (2016). "Effect of environmentally-friendly flame retardants on fire resistance and mechanical properties of rigid polyurethane foams," *Polimery* 61(2), 113-116. DOI: 10.14314/polimery.2016.113

Poletto, M., Zattera, A. J., and Santana, R. M. C. (2012). "Structural differences between wood species: evidence from chemical composition, FTIR spectroscopy, and thermogravimetric analysis," *Journal Applied Polymer Science* 126(1), 337-344. DOI: 10.1002/app.36991

Shao, Q., Li, H. Q., Huang, C. P., and Xu, J. (2016). "Biopolyol preparation from liquefaction of grape seeds," *Journal Applied Polymer Science* 133, 34, 43835. DOI: 10.1002/APP.43835

Sluiter, A., Hames, B., Ruiz, R., Scarlata, C., Sluiter, J., and Templeton, D. (2008a). *Determination of Ash in Biomass* (NREL/TP-510-42622), National Renewable Energy Laboratory, Golden, CO, USA.

Sluiter, A., Hames, B., Hyman, C. P., Payne, C., Ruiz, R., Scarlata, C., Sluiter, J., Templeton, D., and Wolfe, J. (2008b). *Determination of Total Solids in Biomass and Total Dissolved Solids in Liquid Process Samples* (NREL/TP-510-42621), National

Renewable Energy Laboratory, Golden, CO, USA.

Sluiter, A., Ruiz, R., Scarlata, C., Sluiter, J., and Templeton, D. (2008c). *Determination of Extractives in Biomass* (NREL/TP-510-42610), National Renewable Energy Laboratory, Golden, CO, USA.

Song, B., Lu, W. Y., Syn, C. J., and Chen, W. (2009). "The effects on strain rate, density, and temperature on the mechanical properties of polymethylene diisocyanate-based rigid polyurethane foams during compression," *Journal Material Science* 44, 351-357. DOI: 10.1007/s10853-008-3105-0

Ugarte, L., Saralegi, A., Fernández, R., Martín, L., Corcuera, M. A., and Eceiza, A. (2014). "Flexible polyurethane foams based on 100% renewably sourced polyols," *Industrial Crop Production* 62, 545-551. DOI: 10.1016/j.indcrop.2014.09.028

Wang, T. P., Li, D., Wang, L. J., Yin, J., Chen, X. D., and Mao, Z. H. (2008). "Effects of CS/EC ratio on structure and properties of polyurethane foams prepared from untreated liquefied corn stover with PAPI," *Chemical Engineering Research Design* 86, 416-421. DOI: 10.1016/j.cherd.2007.12.002

Wu, J., Wang, Y., Wan, Y., Lei, H., Yu, F., Liu, Y., Chen, P., Yang, L., and Ruan, R. (2009). "Processing and properties of rigid polyurethane foams based on bio-oils from microwave-assisted pyrolysis of corn stover," *International Journal Agricultural & Biology Engineering* 2(1), 40-50. DOI: 10.3965/j.issn.1934-6344.2009.01.040-050

Xie, J., Qi, J., Hse, C.Y., and Shupe, T. F. (2014). "Effect of lignin derivatives in the bio-polyols from microwave liquefied bamboo on the properties of polyurethane foams," *BioResources* 9(1), 578-588. DOI: 10.15376/biores.9.1.578-588

Xie, J., Zhai, X., Hse, C. Y., Shupe, T. F., and Pan, H. (2015). "Polyols from microwave liquefied bagasse and its application to rigid polyurethane foam," *Materials* 8, 8496-8509. DOI: 10.3390/ma8125472

Xie, J., Hse, C. Y., Shupe, T. F., Pan, H., and Hu, T. (2016). "Extraction and characterization of holocellulose fibers by microwave-assisted selective liquefaction of bamboo," *Journal Applied Polymer Sci*ence 133, 18. DOI: 10.1002/app.43394

Xue, B. L., Wen, J. L., and Sun, R. C. (2015). "Producing lignin-based polyols through microwave-assisted liquefaction for rigid polyurethane foam production," *Materials* 8, 586-599. DOI: 10.3390/ma8020586

Xu, J. M., Xie, X. F., Wang, J. X., and Jiang, J. C. (2016). "Directional liquefaction coupling fractionation of lignocellulosic biomass for platform chemicals," *Green Chemistry* 18, 3124-3138. DOI: 10.1039/C5GC03070F

Yan, Y., Pang, H., Yang, X., Zhang, R., and Liao, B. (2008). "Preparation and characterization of water blown polyurethane foams from liquefied cornstalk polyol," *Journal Applied Polymer Science* 110, 1099-1111. DOI: 10.1002/app.28692

Zhang, H., Ding, F., Luo, C., Xiong, L., and Chen, X. (2012a). "Liquefaction and characterization of acid hydrolysis residue of corncob in polyhydric alcohols," *Industrial Crop Production* 39, 47-51. DOI: 10.1016/j.indcrop.2012.02.010

Zhang, H., Pang, H., Shi, J., Fu, T., and Liao, B. (2012b). "Investigation of liquefied wood residues based on cellulose, hemicellulose, and lignin," *Journal Applied Polymer Science* 123(2), 850-856. DOI: 10.1002/app.34521

Zhang, C., and Kessler, M. R. (2015). "Biobased polyurethane foam made from compatible blends of vegetable-oil-based polyol and petroleum-based polyol," *ACS Sustainable Chemical Engineering* 3(4), 743-749.

Zhang, H., Pang, H., Zhang, L., Chen, X., and Liao, B. (2013). "Biodegradability of polyurethane foam from liquefied wood-based polyols," *Journal Polymer Environment* 2(2), 329-334. DOI: 10.1007/s10924-012-0542-2

Zhang, Q., Lin, X., Chen, W., Zhang, H., and Han, D. (2020). "Modification of rigid polyurethane foams with the addition of nano-SiO_2 or lignocellulosic biomass," *Polymers* 12(107), 1-10. DOI:10.3390/polym12010107

Zhao, Y., Yan, N., and Feng, M. (2012). "Polyurethane foams derived from liquefied mountain pine beetle-infested barks," *Journal of Applied Polymer Science* 123(5), 2849-2858. DOI: 10.1002/app.34806

Zhuang, Y., Guo, J., Chen, L., Li, D., Liu, J., and Ye, N. (2012). "Microwave-assisted direct liquefaction of ulva prolifera for bio-oil production by acid catalysis," *Bioresources Technology* 116, 133-139. DOI: 10.1016/j.biortech.2012.04.036

Article submitted: March 24, 2020; Peer review completed: May 31, 2020; Revised version received and accepted: June 12, 2020; Published: June 18, 2020.
DOI: 10.15376/biores.15.3.6061-6079